Time-of-flight atom probe measurements on Ni3Al and Co3W

Soer, W.A.; Bronsveld, Paulus; De Hosson, J.T.M.

Published in:
Ultramicroscopy

DOI:
10.1016/S0304-3991(02)00318-2

Publication date:
2003

Available online at www.sciencedirect.com
SCIENCE DIRECT®
ELSEVIER
Ultramicroscopy 95 (2003) 207–213
ultramicroscopy
www.elsevier.com/locate/ultramic

Time-of-flight atom probe measurements on Ni_3Al and Co_3W

W.A. Soer, P.M. Bronsveld, J.Th.M. De Hosson*

Department of Applied Physics, Materials Science Center, Netherlands Institute for Metals Research, University of Groningen, Nijenborgh 4, 9747 AG Groningen, The Netherlands

Received 1 August 2001; received in revised form 12 December 2001

Abstract

In this study, a VG FIM100 was taken into operation, consisting of a field-ion microscope (FIM), a time-of-flight atom probe (TOFAP) and an imaging atom probe. A tungsten specimen was used to calibrate the conversion of flight times to m/n values. The resulting relative mass resolution of the TOFAP was calculated to be $m/\Delta m \approx 500$ FWHM. In time-of-flight measurements of homemade boron-doped Ni-rich Ni_3Al, a so-called ladder diagram was constructed from the evaporation data of a $\langle 0\,0\,1 \rangle$ pole. This ladder diagram revealed a very high degree of ordering in the alternating pure Ni and mixed Ni/Al planes: only 0.4% of the detected Al atoms were located on pure Ni planes. The number of null pulses to start a new plane was found to be much higher for Ni/Al planes (5×10^2) than for Ni planes (1×10^2). Moreover, the ladder diagram showed that boron was uniformly distributed through the matrix with nearly all boron found on pure Ni-planes. The suggestion that boron preferentially settles on these planes would be supported by reports of a strong Ni–B bond, since on Ni planes, B atoms can be accommodated on octahedral interstitial sites surrounded by only Ni atoms. Finally, we performed time-of-flight measurements on Co_3W. The ion species observed in these measurements included a wide variety of WN_n^{2+} ions, with $0 \leqslant n \leqslant 9$. Especially, the ions with odd n prevailed in this ion group.

PACS: 61.72.S

Keywords: Atom probe field ion microscopy; Ni_3Al; Co_3W

1. Introduction

During the last decades the ordered intermetallic compound Ni_3Al has received considerable attention as both a model material and a structural alloy. The high corrosion resistance and the flow stress behavior make the material very attractive for applications at elevated temperatures. However, practical use was prohibited for a long time by the extreme brittleness of polycrystalline Ni_3Al. In 1979, Aoki and Izumi succeeded in increasing the ductility of polycrystalline Ni_3Al to 35% by doping it with small amounts of boron [1]. Auger studies by Liu et al. [2] indicated that this beneficial effect is caused by grain boundary segregation of the boron addition. Grain boundary observations in 1986 by Horton and Miller using atom probe field-ion microscopy (APFIM) confirmed this preference [3].

*Corresponding author. Tel.: +31-50-363-4898; fax: +31-50-363-4881.

E-mail address: hossonj@phys.rug.nl (J.T.M. De Hosson).

0304-3991/03/$ - see front matter © 2002 Elsevier Science B.V. All rights reserved.
PII: S0304-3991(02)00318-2

With the acquisition of both a scanning Auger microscope and an atom probe field-ion microscope it was decided to look into this topic again based on in situ cracking [4] on homemade material. In this paper we present an APFIM study of the boron distribution in boron-doped Ni-rich Ni_3Al. The atom probe used is a VG FIM100 time-of-flight atom probe (TOFAP). A large part of the experiment was devoted to the control and calibration of the TOFAP; a LabWindows™ program was written for this purpose. In addition to Ni_3Al, we investigated Co_3W to compare its ordered hexagonal $D0_{19}$ structure [5,6] with the ordered cubic $L1_2$ structure of Ni_3Al.

2. Experiment

In a time-of-flight atom probe, field-evaporated specimen ions are taken into a mass spectrometer where they are identified by their time of flight. The TOFAP consists of a so-called Poschenrieder electrostatic lens, which features both spatial and time focusing of the evaporated ions [7,8]. A CAMAC crate contains the timing system of the TOFAP as well as a DAC and an ADC for high-voltage control and readout. Originally, the VG FIM100 came with a control program on a PDP11 computer system. In our experiment we wrote a customized LabWindows program running on a standard PC to control the instrument and fit our own needs. The program communicates with the CAMAC crate through a GPIB™ interface card in the PC and a LeCroy™ 8901A CAMAC-to-GPIB interface module in the crate.

The mass-to-charge ratio m/n is calculated from the measured flight times of the ions. The conversion is based on the equality of the potential energy of the ion at the specimen surface and its kinetic energy at the detector and includes three adjustable parameters to correct for possible non-linear behavior:

$$\frac{m}{n} = 0.19287\alpha(V_{DC} + \beta V_P)\frac{(t - t_0)^2}{d^2},$$

where V_{DC} is the DC tip voltage, V_P is the pulse voltage, t is the flight time in ns and d is the length of the flight path in mm. The factor α corrects for overall losses and deviations associated with the tip voltage; β is introduced to correct for small voltage overshoots and deficits on application of the voltage pulse. To allow for a time delay due to cables and circuits, a correction time t_0 is subtracted from the measured time.

The calibration of the parameters was performed on a tungsten specimen in a neon image gas background using five spectra with a total of 35 peaks. For these peaks the m/n values ranged from 10 for $^{20}Ne^{2+}$ ions to 62 for $^{186}W^{3+}$ ions. Using numerical non-linear curve fitting on these data, the calibration parameters were determined to be $\alpha = 1.054 \pm 0.007$, $\beta = 0.91 \pm 0.04$ and $t_0 = (25 \pm 7)$ ns with a correlation of $R^2 = 0.99998$. From the W^{3+} peak widths, the relative mass resolution achievable with this calibration was determined to be $m/\Delta m \approx 500$ FWHM. In practice, imperfections in the measurement and application of the tip voltage gave rise to small variations in the parameters for measurements under different conditions. However, these imperfections could easily be accounted for by adjusting only α and leaving the other parameters unchanged.

3. Results and discussion

The used Ni_3Al material had been heat-treated using the Gottstein treatment of successive rolling and heat treatment [9], resulting in an average grain size of approximately 100 μm. Because the field-ion microscope (FIM) specimens were several orders of magnitude smaller, we used transmission electron microscopy (TEM) to preselect specimens with favorable grain boundaries. Although grain boundaries were observed in the TEM, they could not be brought to surface by field evaporation in the FIM, as they were still located too far away from the tip end. Smaller-grained Ni_3Al will have to be prepared to overcome this problem, e.g. by [0 0 1] single crystal zone refining and subsequent $\Sigma 3$ and low angle grain boundary introduction by compression as described by Demura et al. [10], or by a method of severe plastic deformation as reported recently by Valiev et al. [11].

The FIM images were in general well resolved and clearly showed the four-fold symmetry associated with the $L1_2$ crystal structure. Fig. 1 shows a $\langle 0\,0\,1 \rangle$ pole, in which a pattern of alternating dim and bright rings can be observed. The pattern consists of rings visualizing the alternating pure Ni and mixed Ni/Al (0 0 2) planes in the $L1_2$-ordered Ni_3Al. Since Al atoms give much more image contrast than Ni atoms, the mixed planes appear as bright rings in the FIM image [3]. As for the TOFAP analysis, Fig. 2 shows a typical m/n spectrum of a Ni_3Al specimen, from which the composition of the analyzed material was determined to be 75.4Ni–23.9Al–0.8B. This is in very good agreement with the overall composition 75.2Ni–24.0Al–0.8B of the bulk material of which the specimen was made.

Besides composition determination, the TOFAP measurements can also be used to analyze the distribution of elements in the material, because the detected ions are stored in order of impact. The alternation of Ni and Ni/Al planes in the $\langle 0\,0\,1 \rangle$ direction mentioned before can be demonstrated in a very elegant way [3]: by collecting ions from a $\langle 0\,0\,1 \rangle$ pole at a slow rate, one detects alternately the atoms from the Ni planes and the Ni/Al planes. When the evaporated Al atoms are now plotted versus the Ni atoms according to their order of impact, a so-called ladder diagram is constructed as shown in Fig. 3. Starting at the origin, the line is drawn horizontally when a Ni ion is detected and vertically when an Al ion is detected. Thus, horizontal lines in the diagram represent pure Ni planes in the crystal, while the diagonal parts represent mixed Ni/Al planes. The diagram reveals a high degree of ordering in the material: only 2 out of 530 measured Al atoms were located on pure Ni planes, which corresponds to a fraction of 0.4%. In addition, the number of null pulses for each ion is plotted in the figure. The nulls/ion curve shows peaks at regular intervals; each of the peaks can be seen to coincide with the beginning of the evaporation of a new plane. The peaks arise because when a new plane is to be

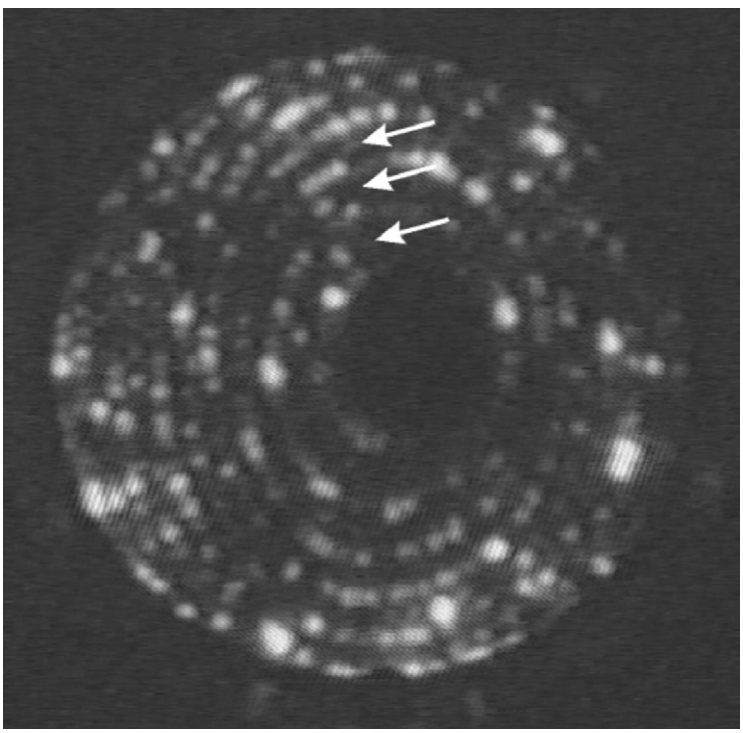

Fig. 1. FIM image of $\langle 0\,0\,1 \rangle$ pole in Ni_3Al. Dim rings are marked with arrows. The dark spot in the center is the hole in the mirror. $V_{DC} = 8.3\,kV$, $T = 50\,K$, $p_{Ne} = 10^{-5}\,mbar$. Recorded with CCD camera on videotape.

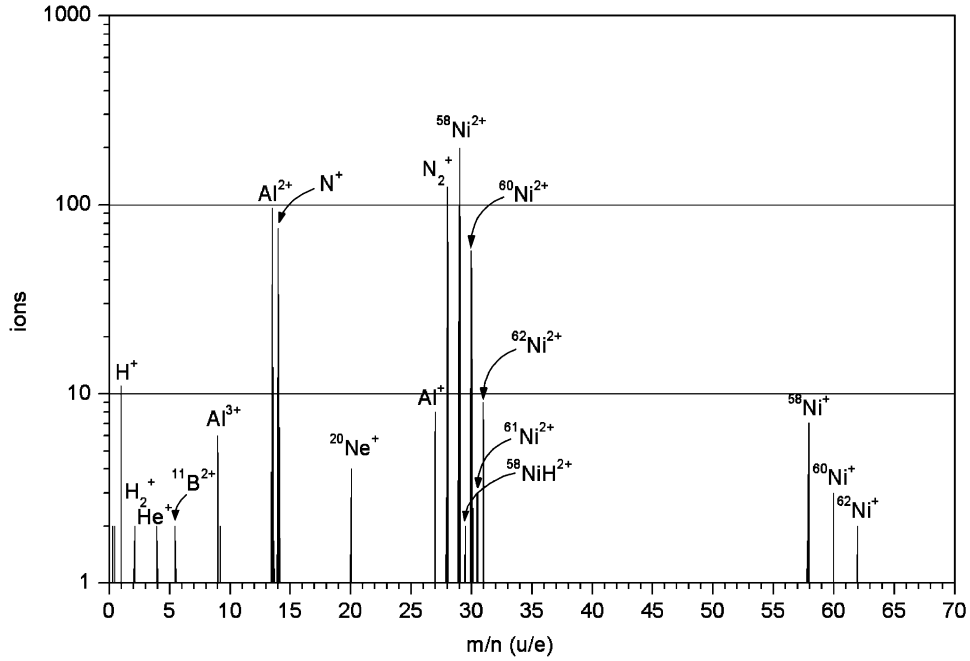

Fig. 2. Spectrum of a Ni3Al specimen at a Ne pressure of 10^{-5} mbar. $V_{DC} = 6.8\,\text{kV}, f_p = 20\%$, $T = 50\,\text{K}$, 997 ions collected in 21 min.

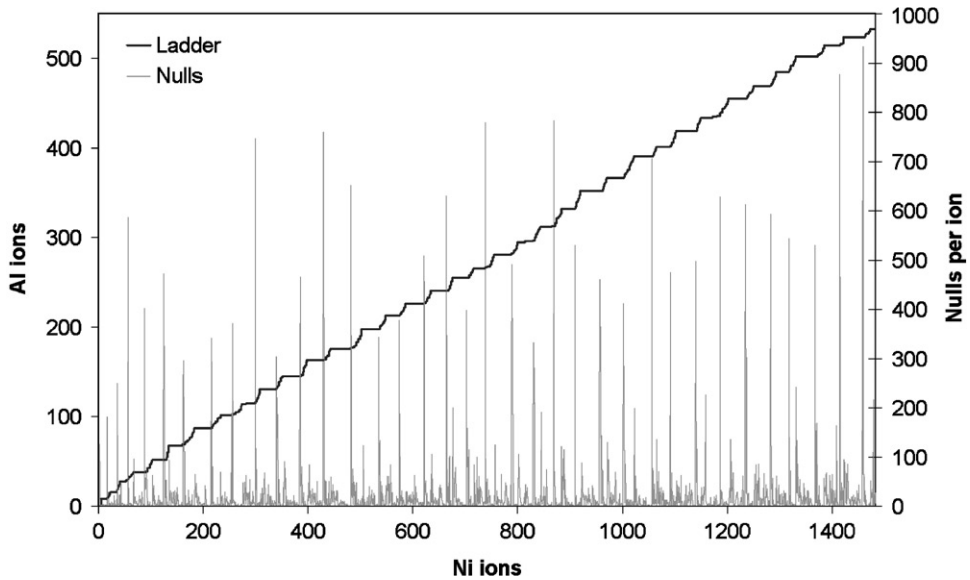

Fig. 3. Ladder diagram of evaporation of Ni_3Al in $\langle 0\,0\,1 \rangle$ direction. $V_{DC} = 7.4\,\text{kV}$, $f_p = 20\%$, $T = 50\,\text{K}$, 2541 ions collected in 142 min.

evaporated, the tip surface is smooth and none of the atoms is exposed to a higher field; however, when a plane is already partly evaporated, atoms are removed much easier due to their enhanced local field. Furthermore, the number of nulls needed to break open a Ni/Al plane (average $(5\pm2)\times10^2$), was generally higher than for a Ni plane (average $(1\pm0.6)\times10^2$); apparently the evaporation field of Ni/Al planes was higher than that of Ni planes under the conditions in our measurement.

It is interesting to compare these results with those by Wanderka et al. [12] and Van Bakel et al. [13]. They both discuss the translation of ion counts into composition on an individual plane basis. For example, Van Bakel reports that the extent of the interruption associated with the transition from a pure nickel plane to a mixed nickel–aluminum plane is not significantly different from the reverse transition. This was in reaction to a previous report by Grüne et al. [14] that the concentration could possibly be dependent on the direction of the transition going from pure Ni to mixed Ni/Al planes or vice versa. That turns out not to be the case, in those two reports nor in this study. Van Bakel plotted the total number of ions in order to get the transition point to a new plane type; in this paper the number of nulls are plotted as indicated in Fig. 3. Making use of the nulls count in order to determine the start of a new plane as applied in this paper may be worth noticing. The plane transition is then well established and, in agreement with the result of Wanderka et al., slow and fast evaporating planes are detected corresponding to mixed and pure planes, respectively.

Besides the information about the Ni_3Al ordering, the ladder diagram provides useful information on the location of other elements in the matrix, especially boron in our case. In Fig. 4, the detected boron atoms are shown as small triangles superposed on part of the ladder diagram of Fig. 3. The boron atoms are uniformly distributed along the ladder diagram. More than a confirmation of our FIM observations that no boron-decorated grain boundaries were present in the analyzed part of the material, this result proves that boron is distributed equally through the matrix. Throughout the entire measurement, 17 out of 20 boron atoms were found to be located on Ni planes and only 3 resided in Ni/Al planes. Although the detected amount of boron is too low to draw any definite conclusions on statistical grounds, the measurements suggest a preference of

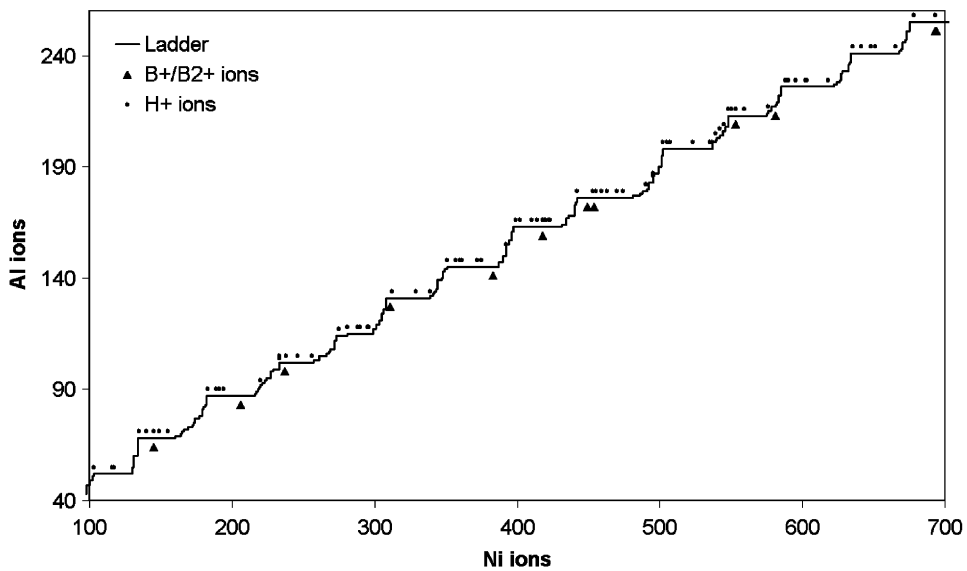

Fig. 4. Detected B and H ions superposed on part of the ladder diagram of Fig. 3.

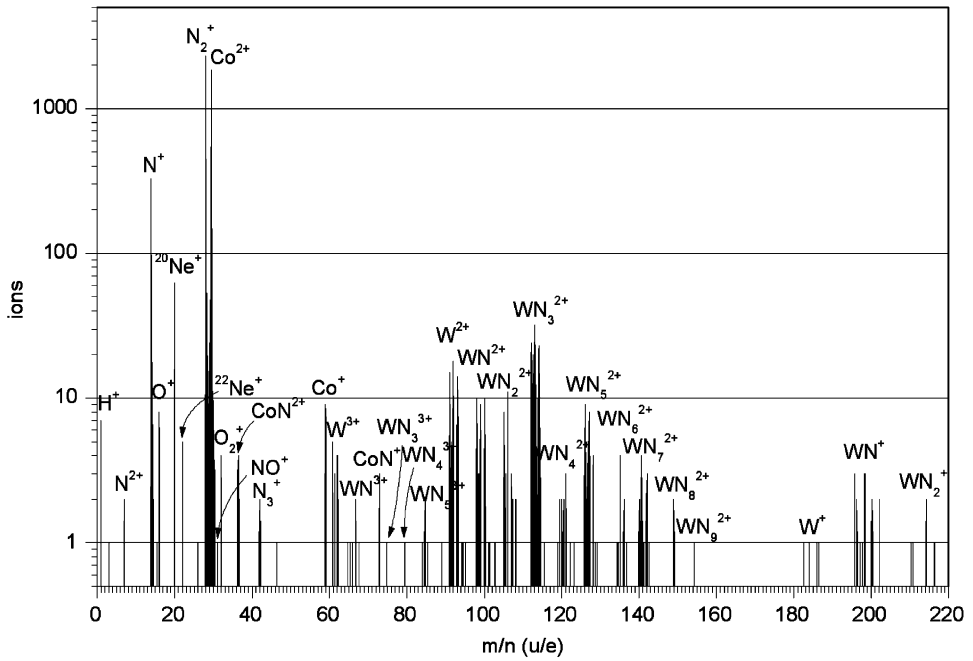

Fig. 5. Spectrum of a Co_3W specimen at a Ne pressure of 5×10^{-7} mbar. $V_{DC} = 12.2$ kV, $f_p = 20\%$, $T = 50$ K, 5307 ions collected in 70 min.

boron in the Ni_3Al matrix to settle on Ni planes. This suggestion is supported by reports of a strong Ni–B covalent bond [15], since on Ni planes, boron atoms can be accommodated on octahedral interstitial sites surrounded by only Ni atoms. Further, TOFAP analysis with more statistical data is recommended to confirm and clarify these observations. A neutron depth profiling (NDP) experiment on the same sample indicated that at least up to a depth of 0.5 μm, the B content had the same constant value [16].

In situ cracking scanning Auger measurements on this specimen [4] showed hardly any boron on the grain boundaries immediately after fracture. However, after the sample had been left in the UHV environment for 24 h, small peaks of B, O and C were observed. The fact that the TOFAP did not indicate oxygen or carbon suggests that those elements were due to contamination while B appeared to have diffused to the surface from the bulk material.

As for the Co_3W material, one of the electrochemically polished specimens showed no ordering in the FIM image, but was suitable for TOFAP measurements. Fig. 5 shows a Co_3W spectrum from which the Co/W ratio of the analyzed part of the specimen was determined to be 1931:490 = 3.94. This high cobalt content is a possible cause of the lack of ordering observed in the FIM image. An interesting aspect of the spectrum was the predominance of complex ions, showing a wide variety of tungsten nitride ion clusters. Most of them were detected in the form of WN_n^{2+} ions, where $0 \leqslant n \leqslant 9$. Especially, the ions with an odd number of N atoms (n) prevailed in this complex ion group. This is a remarkable observation, since a previous study on adsorption of N_2 on tungsten did not report this preference [17]. Further research may be required at this point, as even more recent publications about the structure of these metal nitride precursor species still describe these clusters as being magic [18].

4. Conclusions

In this experiment, a time-of-flight atom probe was successfully operated and calibrated. TOFAP

measurements on B-doped Ni_3Al showed boron to be distributed over the whole matrix with a preference for pure Ni planes. In a Co_3W spectrum a wide variety of WN_n^{2+} ions were found. Double charged complex ions with odd n were favored over ions with even n.

Acknowledgements

We gratefully acknowledge the continuous contact by e-mail with A. Cerezo, A.W. Waugh and S.J. Sijbrandij. The confidence in our efforts by H. Rogalla was of crucial importance. Frequent discussions with J.B. Kuipers helped us to understand and tackle digitized video signals.

LabWindows and GPIB are registered trademarks of National Instruments Corporation. LeCroy is a registered trademark of LeCroy Corporation.

References

[1] K. Aoki, O. Izumi, Nippon Kinzoku Gakkaishi 43 (1979) 1190.
[2] C.T. Liu, C.L. White, J.A. Horton, Acta Metall. 33 (1985) 213.
[3] J.A. Horton, M.K. Miller, Acta Metall. 35 (1987) 133.
[4] S.A. Koch, D.T.L. Van Agterveld, G. Palasantzas, J.Th.M. De Hosson, Surf. Sci. Lett. 476 (2001) L267.
[5] P.A. Carvalho, H.S.D. Haarsma, B.J. Kooi, P.M. Bronsveld, J.Th.M. De Hosson, Acta Mater. 48 (2000) 2703.
[6] S. Ranganathan, Philos. Mag. 19 (1969) 415;
S. Ranganathan, Surf. Sci. 20 (1970) 429.
[7] W.P. Poschenrieder, Int. J. Mass Spectrom. Ion Phys. 6 (1971) 413;
W.P. Poschenrieder, Int. J. Mass Spectrom. 9 (1972) 357.
[8] E.W. Müller, S.V. Krishnaswamy, Rev. Sci. Instrum. 45 (1974) 1053.
[9] C. Escher, G. Gottstein, Acta Mater. 46 (1998) 525.
[10] M. Demura, Y. Suga, O. Umezawa, K. Kishida, E. George, T. Hirano, Intermetallics 9 (2001) 157.
[11] R.Z. Valiev, C. Song, S.X. McFadden, A.K. Mukherjee, R.S. Mishra, Philos. Mag. A 81 (2001) 25.
[12] N. Wanderka, U. Glatzel, Mater. Sci. Eng. A 203 (1995) 69.
[13] G.P.E.M. Van Bakel, K. Hariharan, D.N. Seidman, Appl. Surf. Sci. 90 (1995) 95.
[14] R. Grüne, A. Hütten, L. Van Alvensleben, Colloq. Phys. C 7 (1986) 295.
[15] G.S. Painter, C.L. Fu, F.W. Averill, J. Appl. Phys. 81 (5) (1997) 2135.
[16] L.H.M. Krings, Y. Tamminga, J. Van Berkum, F. Labohm, A. Van Veen, W.M. Arnoldbik, J. Vac. Sci. Technol. A 17 (1) (1999) 198.
[17] E.W. Muller, T.T. Tsong, Prog. Surf. Sci. 4 (1) (1973) 33.
[18] S.E. Kooi, A.W. Castleman Jr., Chem. Phys. Lett. 315 (1999) 49.